D. Sitarski

R. J. Lee

J. R. Saylor
e-mail: jsaylor@clemson.edu

Department of Mechanical Engineering,
Clemson University,
Clemson, SC 29634

John P. McHugh
Department of Mechanical Engineering,
University of New Hampshire,
Durham, NH 03824
e-mail: john.mchugh@unh.edu

Large-Scale Circulation in a Rectangular Enclosure With Periodic Boundary Temperature

An experiment in a rectangular basin of water is used to demonstrate that a large-scale circulation will result from a zero-mean thermal forcing. The thermal force is a spatially periodic pattern of heating and cooling at the top surface, achieved with an interdigitated array of hot and cold tubes. The experimental results show a very robust, steady flow with ascending flows at each end of the tank and a single descending jet near the left wall. These results suggest that small-scale forcing in surface-driven flows may result in significant large-scale subsurface motion. [DOI: 10.1115/1.4024011]

1 Introduction

The work presented here falls within the broad category of natural convection in cavities. This subject has a long history of experimental, analytical, and numerical study that has treated a wide range of configurations. Previous cases with rectangular cavities have generally used heating or cooling that is uniform across each surface, such as Rayleigh–Bénard convection [1–3], which has uniform heating along the bottom and uniform cooling along the top. Another important configuration is differential heating on the cavity sides, with uniform heating along one vertical wall and uniform cooling along the opposite wall [4–6]. Each style of boundary heating has in turn been subject to further permutations, including the imposition of constant temperature versus constant heat flux boundary conditions [7], and temporal variations in the boundary forcing. Applications of these results include the design of solar energy collectors, cooling of electronic equipment, air flow in buildings, geophysical flows, and more.

The present work treats natural convection experiments in a cavity with heating and cooling only at the top boundary. The boundary heating here is chosen to be spatially periodic in such a way that the average surface temperature is identical to the ambient. This type of thermal forcing is quite different from situations where a mean temperature difference that is statically unstable is imposed; here the mean temperature difference is zero.

The results of the present experiments find application in any situation where thermal forcing occurs at one horizontal boundary and where there are spatial variations in the thermal forcing. While a sinusoidal forcing pattern is chosen here, the general phenomenon which is observed (namely a basin scale flow) is expected to exist for other zero mean, spatially nonuniform forcings as well. Examples where such flows can exist include small lakes, cooling ponds, crystal growth from melts [8,9] and others. Another possible application is larger geophysical bodies, such as the oceans [10–12]. The oceans are also heated and cooled from above but are very shallow compared to the horizontal dimension and also are significantly influenced by the Coriolis effect. The experiments considered here have a much different aspect ratio than the oceans, and rotation is insignificant, however the results given here show a relationship between fluctuations in boundary forcing and basin-scale motion, and a similar relationship may exist in oceanic flow.

Contributed by the Fluids Engineering Division of ASME for publication in the Journal of Fluids Engineering. Manuscript received September 6, 2011; final manuscript received January 7, 2013; published online April 17, 2013. Assoc. Editor: Mark F. Tachie.

In addition to thermal forcing, cavity flow may be driven by mechanical forcing at one or more boundaries [13]. The vast majority of these cases have treated rectangular cavities with forcing that is unidirectional across one or more surfaces of the cavity, with the most common choice being constant forcing across the top. This choice of constant force implicitly assumes that fluctuations in boundary forcing would average to zero and have no impact on the overall flow. However, recent simulations [14] have shown that a surface force that alternates direction such that the mean is zero can also cause large-scale motion in the cavity. This result violates conventional wisdom by suggesting that the effect of the fluctuations in surface forcing does not merely average to zero, but may be as important as the prevailing effect.

The aforementioned simulations showing how spatially periodic mechanical forcing can cause basin-scale motion [14] suggest that thermal forcing may have a similar behavior. This motivates the present work where experiments are presented with a spatially periodic thermal forcing at the top of a basin of water to demonstrate that these oscillations can indeed drive a large-scale mean flow. The forcing is an imposed, spatially periodic temperature. Although this spatially periodic temperature (and hence buoyancy) was used as the forcing here, the results also provide some experimental validation of the previous computations [14].

The present experiments may appear similar to the well-known work of Rossby [15,16] (and earlier studies by Stommel [17]) who investigated the flows generated by a linear temperature profile at the bottom of a water basin. Rossby [15,16] did observe a basin filling flow like that seen here. However, the forcing in Rossby's experiments was a *constant* temperature gradient across the tank bottom, which is analogous to cases with uniform surface force [13]. As the forcing in Rossby's work is statically unstable, the results are not directly relevant to the present results.

In the present experiments, the temperature at the surface has eight oscillations, similar in concept to the $n = 16$ case of Osman et al. [14], shown in Fig. 1, where a sinusoidally varying surface velocity was imposed. Osman et al. used direct numerical simulations and showed that spatial oscillations in surface velocity result in a basin-scale flow at the bottom of the basin, even when the force has a zero mean and the flow is laminar and steady. The resulting flow exhibited either a subcritical or supercritical bifurcation to steady asymmetric flow, depending on the length-scale of the forcing, the Reynolds number, and the aspect ratio of the cavity [14,18]. The basin-scale motions appeared in the asymmetric flow as can be seen in the streamlines presented in Fig. 1. Figure 1 also reveals that the effect of the spatial periodicity in the forcing is relegated to only the upper portion of the fluid domain.

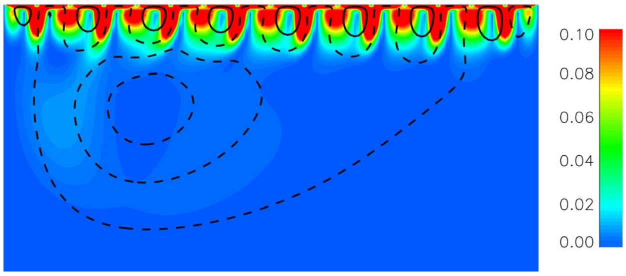

Fig. 1 Basin scale flow observed in the numerical work of Osman et al. [14]. (Reprinted.) The lines are streamlines: solid streamlines indicate clockwise rotation, and dashed streamlines indicate counterclockwise rotation. The solid-fill shading represent contours of the magnitude of velocity normalized by the magnitude of the forcing velocity.

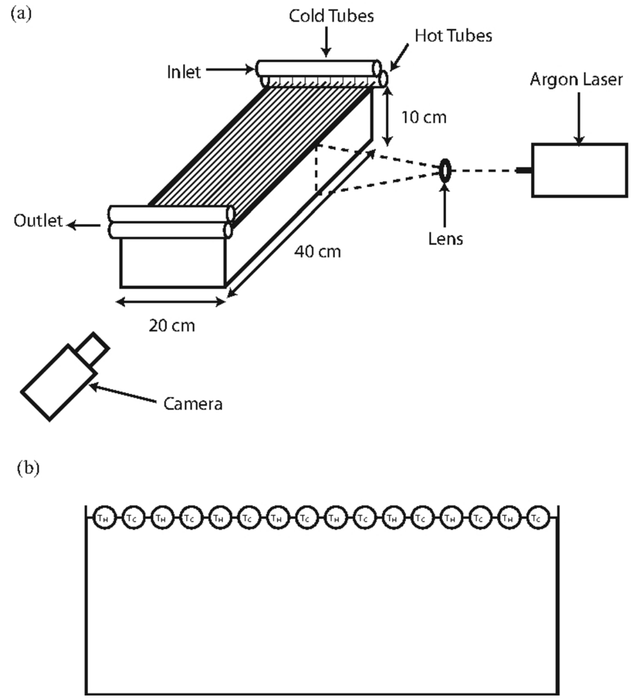

Fig. 2 Schematic of (*a*) the experimental setup showing the location of the hot and cold manifolds at the tank ends, and (*b*) a cross section of the tank showing the pattern of hot and cold tubes. The pattern of lines in (*a*) connecting the inlet and outlet manifolds represent the tubes shown in (*b*).

In the numerical simulations of Osman et al. the sinusoidal forcing was of the form

$$U(x) = \sin n\pi x \tag{1}$$

where $0 \le x \le 1$, and the forcing mode number, n, was chosen to be an even positive integer so that the mean force was zero. For cases where the length-scale of the forcing was small relative to the depth of the cavity (large n), the flow in the bottom of the cavity developed a basin-filling flow, much different than the flow at the top near the forcing boundary. The particular case with $n = 16$ in a rectangular cavity showed a flow pattern very similar to the case with constant forcing, except near the forcing boundary. This asymmetric flow resulted after a bifurcation from a symmetric flow at a Reynolds number of approximately 900, where the Reynolds number is defined as

$$R_e = \frac{UL}{\nu} \tag{2}$$

where U is the magnitude of the forcing velocity, L is the (horizontal) width of the cavity, and ν is the kinematic viscosity. The velocities in the present experiments were on the order of 1 mm/s with a maximum of approximately 5 mm/s (as shown later), giving a Reynolds number as large as $R_e = 1150$, which is on the same order as R_e for the results in Fig. 1.

The results provided here confirm that periodic thermal forcing at the top can result in basin-scale flows. However symmetric steady flow was never achieved, and the critical heating level for the transition to asymmetric basin-scale motion could not be determined. Apparently this transition occurs at very low forcing temperatures that were not explored herein. Section 2 of this paper provides the basic experimental details, Sec. 3 presents the results, and finally Sec. 4 states the conclusions.

2 Experimental Setup

The present experiments were conducted in a water tank which is illustrated in Fig. 2. The tank is constructed of glass with dimensions $H = 10$ cm, $L = 20$ cm, and $D = 40$ cm, where H is the height, L is the length, and D is the span of the tank. The aspect ratio of the tank therefore is $L/H = 2$, matching Osman et al. [14], Fig. 1.

The periodic variation in temperature at the top of the tank shown in Fig. 2 was achieved with two tube arrays. Hot water flowed through one of the arrays, and cold water through the other. The tube arrays were interdigitated so that alternately hot and cold tubes lay upon the water surface. Each set of tubes was connected to a pair of manifolds at each end of the tank, which in turn were connected to the inlet and outlet of separate constant temperature water baths set at the desired temperature. Water was forced through each set of tubes by a pump located in each water bath. Each pump had a flow rate of 12 l/min (±1.5 l/min). The temperature in each bath was monitored with a thermocouple. The goal of this arrangement was to impose a temperature at the boundary (rather than a flux) that varies with position but is constant in time. As with all heat transfer experiments, imposing a perfect constant temperature boundary condition is not possible. Heat transfer from the tubes to the tank water will result in slight changes in temperature along the length of the tube. However, due to the high flow rate through the tubes and small velocities in the tank, this effect is expected to be minor. Furthermore, as shown below, the experimental results were very insensitive to small changes in the experimental setup, and the effect of slight changes in the tube temperature along its length is not expected to be significant.

The results presented here were obtained with the fluid flowing through the hot tubes set to a temperature (T_h) of 12, 10, 8, 6, and 4 K above ambient (which was typically around 23 °C), and the temperature of the cold tubes (T_c) set to a temperature 12, 10, 8, 6, and 4 K below ambient. The temperature difference is characterized with

$$\Delta T = T_h - T_c \tag{3}$$

Hence three cases were considered, $\Delta T = 24$, 20, 16, 12, and 8,K. The tube diameter is $\frac{1}{4}$ in.

The flow field was acquired using a streakline imaging method. The flow was seeded with rhodamine-B impregnated polystyrene latex spheres. Fluorescence from these spheres was excited using an argon ion laser (500 mW, all lines mode), formed into a sheet using a cylindrical lens. The laser sheet was located halfway between the end-walls of the tank, and filled the entire depth of the tank except for the top 2 cm of the tank where the sheet was blocked by the tube manifold. Images were collected with a Cooke Scientific digital camera (SensiCam) using a multiple

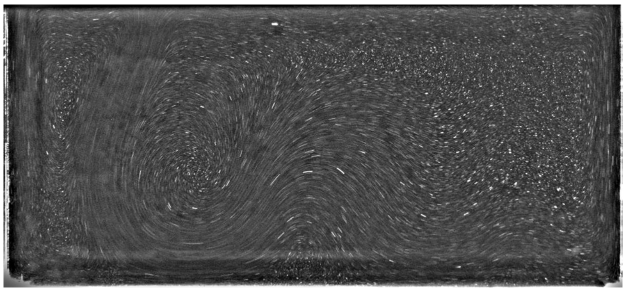

Fig. 3 Streaklines obtained using the apparatus presented in Fig. 2 for the $\Delta T = 8$K case. Fourier filtering and contrast enhancement was used to better reveal the particles.

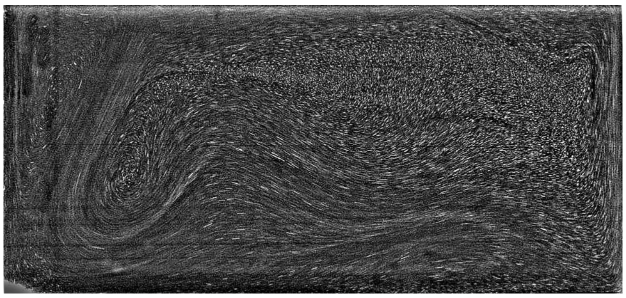

Fig. 4 Streaklines obtained using the apparatus presented in Fig. 2 for the $\Delta T = 12$K case. Fourier filtering and contrast enhancement was used to better reveal the particles.

exposure mode so that a particle that remained in the laser sheet was imaged several times creating a streak of closely spaced dots. An image was acquired by obtaining 40 multiple exposures each of 1 ms duration and separated by approximately 100 ms, giving a total exposure time for each image of 4.04 s.

3 Results

The experiment is initiated from rest by starting the flow of hot and cold water through the tubes. The bulk temperature of the water in the tank was initially in equilibrium with the ambient. There is a transient period during which the bulk water temperature decreases to a value $\sim 2-3$K below room temperature and during which the flow field changes. Steady state in the fluid flow was assumed to exist when the flow field did not appear to be changing and when the decline in temperature in the tank was less than 0.2 °C in a 50 min period. This typically occurred within 3 h, after which image acquisition began.

Experiments were conducted with $\Delta T = 8, 12, 16, 20$, and 24K. The flow pattern that existed once steady state was achieved for each of these cases is shown in Figs. 3–7. The entire flow is imaged in these figures except for the very top of the tank. Notice that in all cases the flow pattern is dominated by a large-scale circulatory flow with a strong vertical jet located about one-fifth of a tank width from the left boundary. This jet is a downward flow, and is the only downward current in the image, while a strong upward current hugs the left and right walls of the tank. The general direction of flow was the same for all cases, and is indicated in the schematic in Fig. 8. The only region of the basin that is not entrained into the basin-scale motion is the narrow region on the left-hand side of the basin. This region appears to exhibit a closed circulation, and includes the upward boundary layer on the left wall of the basin.

A close examination of the images in Figs. 3–7 reveals that near the top of the tank, there is an oscillation whose wavelength is commensurate with the spacing of the hot and cold tubes, most clearly visible in Fig. 7. The top 2 cm of the tank are blocked by

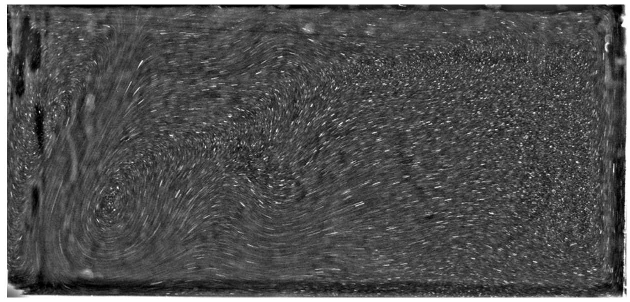

Fig. 5 Streaklines obtained using the apparatus presented in Fig. 2 for the $\Delta T = 16$K case. Fourier filtering and contrast enhancement was used to better reveal the particles.

Fig. 6 Streaklines obtained using the apparatus presented in Fig. 2 for the $\Delta T = 20$K case. Fourier filtering and contrast enhancement was used to better reveal the particles.

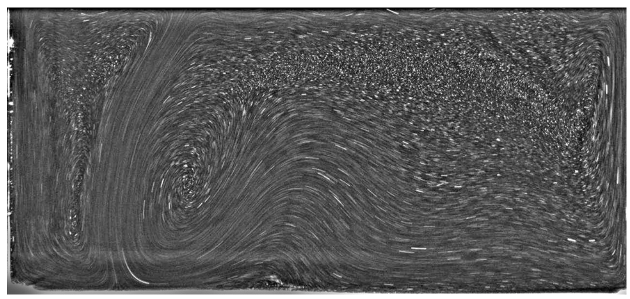

Fig. 7 Streaklines obtained using the apparatus presented in Fig. 2 for the $\Delta T = 24$K case. Fourier filtering and contrast enhancement was used to better reveal the particles.

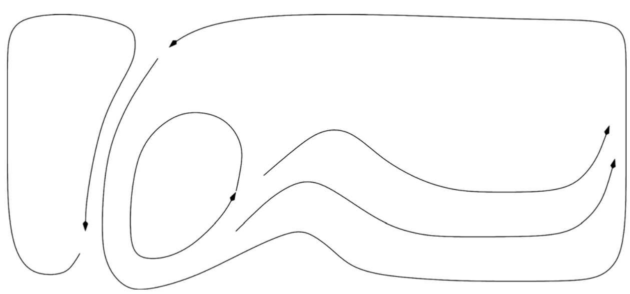

Fig. 8 Schematic showing the direction of flow

tubing, as mentioned previously, and is not visible in these images. It is likely that the flow pattern in this top region is dominated by the length-scale of the tubing spacing, similar to the results of Osman et al. [14]. The pattern that emerges in the present experiments shares the overall character of a bulk circulation that is present in the results of Osman et al., but the details of the two flows are different. In particular, the present experiments show a nearly vertical jet that does not appear in the computations of Osman et al.

The experiments show that there is a consistent overall flow pattern for all temperature differences, clearly present in Figs. 3–7. This flow pattern is extremely robust once a steady-state condition is attained. Repeated trials on different days show the same flow, even after the tank is emptied, cleaned, and refilled. It is noted that the hot and cold tube arrays were manually put in place each time the tank was cleaned and refilled. While great care was taken to place these arrays in the same place each time, it is likely that the positions differed by a millimeter or two from experiment to experiment. In spite of this, the flow pattern was still very similar from run to run. The flow pattern is not symmetric about the tank centerline, despite the symmetry of the boundary temperature. The previous results of Osman et al. [14] showed a flow pattern that was symmetric about the tank centerline at very low Reynolds numbers. As the Reynolds number was increased in subsequent trials, the flow pattern became strongly asymmetric. A similar symmetric flow was expected in the present experiments with small ΔT but did not appear. Instead for all cases only the asymmetric pattern shown in Figs. 3–7 was present. Apparently the symmetric flow and the transition to asymmetric flow happens at very low values of ΔT. Such low temperature differences could not be accurately attained in this experimental setup and the parameter values for the transition from symmetric to asymmetric flow could not be determined.

The speeds of the downward jet and the upward jet on the right-hand side of the image were obtained by measuring the length of the streaks in the image and dividing by the exposure time. These velocities are plotted in Fig. 9 for cases with forcing temperatures of $\Delta T = 8, 16,$ and 24K. Only the brightest streaks that clearly show the endpoints of the streak are included in these measurements. Because of the scarcity of streaks, the streaks were not all obtained at the same physical location; any good streaks located in the jets were used to obtain the jet velocity averages plotted in Fig. 9. The number of streaks used to obtain the six values presented in Fig. 9 ranged from 6 to 15, with an average of 10. The vertical bars in the figure are the 95% confidence intervals based on the scatter in the data and the effect of pixelization error on the velocity measurement. The results in Fig. 9 show the jet velocities increase with ΔT in subsequent trials. Note that this increase in flow speed is not linear. Because the velocity in the jet changes with ΔT it is almost certainly the case that the velocity in other areas of the tank also change with ΔT. This means that the flow pattern is staying the same, even as the fluid moves about at a more rapid pace.

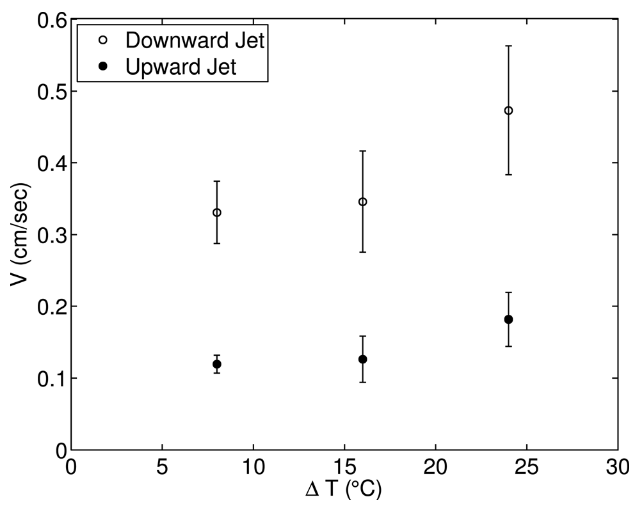

Fig. 9 Velocities in the downward and upward jet. Each point is the average of the measurements obtained in the jet at ΔT. The vertical bars are 95% confidence intervals.

4 Conclusions and Discussion

This experiment demonstrates that a small-scale forcing can result in a large-scale flow that does not retain the forcing length-scales. These results suggest that perhaps large-scale currents in geophysical bodies of water and cooling ponds are affected significantly not only by the prevailing effect, but by the smaller scale forcing, even if this smaller scale forcing has a zero mean.

Here we provide a physical explanation of the large-scale flow that, while not conclusive, is in agreement with the observations. Shortly after initiation of the experiment, the hot and cold tubes cause the nearby water in the tank to also be hot or cold, while the remainder of the tank is still at ambient temperature. The hot water near the tubes will move upward due to buoyancy effects while the cold fluid will move downward. But the upward motion of the hot water is limited by the immediately adjacent top boundary, while the downward motion of the cold water is only limited by the more distant bottom boundary. As a result, shortly after initiation, there is a layer of water a short distance beneath the top boundary that has an average temperature that is less than ambient, and therefore a statically unstable state has emerged. This initiates the overturning motion that appears in the experiments. Once this motion has begun, the influence of the warm tubes is limited, as they do not act to stop the motion. It may be that the streamlines near the warm tubes are closed, and this warm fluid does not mix with the remainder of the water, while the cold water is constantly being circulated. This favoritism for cold water apparently provides the buoyant force that maintains the steady motion. This mechanism may also explain why the steady-state bulk temperature in the tank was slightly lower than the ambient temperature.

Finally, we note an interesting complement to the present work, namely studies of turbulent Rayleigh–Bénard convection. In Rayleigh–Bénard convection, a fluid is confined between two horizontal plates, the lower having a higher temperature than the upper. In such experiments, the driving force acts in the vertical direction, and no preference should exist for a circulatory flow or any large scale horizontal motion. Nevertheless, even at very high Rayleigh numbers, several investigators have found that a basin-scale circulation or "wind" exists [19–23]. This circulation remains despite careful attention to the uniformity of forcing and the orientation of the experimental apparatus. These results show that a uniform thermal boundary condition results in a basin-filling flow. These previous results along with the present results may imply that a basin-filling flow will appear under most conditions.

References

[1] Rayleigh, L., 1916, "On Convection Currents in a Horizontal Layer of Fluid, When the Higher Temperature is on the Under Side," Philos. Mag., **32**, pp. 529–546.
[2] Koschmieder, E. L., 1993, *Bénard Cells and Taylor Vortices*, Cambridge University Press, Cambridge, UK.
[3] Bodenschatz, E., Pesch, W., and Ahlers, G., 2000, "Recent Developments in Rayleigh-Bénard Convection," Annu. Rev. Fluid Mech., **32**, pp. 709–778.
[4] Trias, F. X., Gorobets, A., Soria, M., and Oliva, A., 2010, "Direct Numerical Simulation of a Differentially Heated Cavity of Aspect Ratio 4 With Rayleigh Numbers Up to 10^{11}—Part I: Numerical Methods," Int. J. Heat Mass Transfer, **53**, pp. 665–673.
[5] Cheikh, N. B., Beya, B. B., and Lili, T., 2007, "Aspect Ratio Effect on Natural Convection Flow in a Cavity Submitted to a Periodical Temperature Boundary," ASME J. Heat Transfer, **129**(8), pp. 1060–1068.
[6] Trias, F. X., Soria, M., Oliva, A., and Pereza-Segarra, C. D., 2007, "Direct Numerical Simulations of Two- and Three-Dimensional Turbulent Natural Convection Flows in a Differentially Heated Cavity of Aspect Ratio 4," J. Fluid Mech., **586**, pp. 259–293.
[7] Verzicco, R., and Sreenivasan, K. R., 2008, "A Comparison of Turbulent Thermal Convection Between Conditions of Constant Temperature and Constant Heat Flux," J. Fluid Mech., **595**, pp. 203–219.
[8] Wüest, A., and Lorke, A., 2002, "Small-Scale Hydrodynamics in Lakes," Annu. Rev. Fluid Mech., **35**, pp. 373–412.

[9] Kumar, V., Basu, B., Enger, S., Brenner, G., and Durst, F., 2003, "Role of Marangoni Convection in Si-Czochralski Melts, Part I: 3D Predictions Without Crystal," J. Cryst. Growth, **253**, pp. 142–154.
[10] McWilliams, J. C., and Restrepo, J. M., 1999, "The Wave-Driven Ocean Circulation," J. Phys. Oceanogr., **29**, pp. 2523–2540.
[11] Whitehead, J. A., 1995, "Thermohaline Ocean Processes and Models," Annu. Rev. Fluid Mech., **27**, pp. 89–113.
[12] Wunsch, C., and Ferrari, R., 2004, "Vertical Mixing, Energy, and the General Circulation of the Oceans," Annu. Rev. Fluid Mech., **36**, pp. 281–314.
[13] Shankar, P. N., and Deshpande, M. D., 2000, "Fluid Mechanics in the Driven Cavity," Annu. Rev. Fluid Mech., **32**, pp. 93–136.
[14] Osman, K. B., McHugh, J. P., and Wei, T., 2008, "Patterns in Surface Driven Flows," Phys. Fluids, **20**(10), p. 103602.
[15] Rossby, H. T., 1965, "On Thermal Convection Driven by Non-Uniform Heating From Below: An Experimental Study," Deep-Sea Res., **12**, pp. 9–16.
[16] Rossby, T., 1998, "Numerical Experiments With a Fluid Heated Non-Uniformly From Below," Tellus, **50**, pp. 242–257.
[17] Stommel, H., 1962, "On the Smallness of the Sinking Regions in the Ocean," Proc. Natl. Acad. Sci., **48**, pp. 766–772.
[18] Farias, J. E., and McHugh, J. P., 2002, "The Symmetric Driven Cavity," Phys. Fluids, **14**, pp. 3179–3188.
[19] Niemela, J. J., Skrbek, L., Sreenivasan, K. R., and Donnelly, R. J., 2000, "Turbulent Convection at Very High Rayleigh Numbers," Nature, **404**, pp. 837–840.
[20] Niemela, J. J., Skrbek, L., Sreenivasan, K. R., and Donnelly, R. J., 2001, "The Wind in Confined Thermal Convection," J. Fluid Mech., **449**, pp. 169–178.
[21] Krishnamurti, R., and Howard, L. N., 1981, "Large-Scale Flow Generation in Turbulent Convection," Proc. Natl. Acad. Sci., **78**, pp. 1981–1985.
[22] Qiu, X. L., and Tong, P., 2001, "Large-Scale Velocity Structures in Turbulent Thermal Convection," Phys. Rev. E, **64**(3), p. 036304.
[23] Ciliberto, S., Cioni, S., and Laroche, C., 1996, "Large-Scale Flow Properties of Turbulent Thermal Convection," Phys. Rev. E, **54**, pp. R5901–R5904.